# Well-Defined Nanoclusters as Fluorescent Nanosensors: A Case Study on $Au_{25}(SG)_{18}$

*Zhikun Wu,* Man Wang, Jiao Yang, Xiaohong Zheng, Weiping Cai, Guowen Meng, Huifeng Qian, Huimin Wang, and Rongchao Jin**

*The fluorescence of nanoparticles has attracted much attention in recent research, but in many cases the underlying mechanisms are difficult to evaluate due to the polydispersity of nanoparticles and their unknown structures, in particular the surface structures. Recent breakthroughs in the syntheses and structure determinations of well-defined gold nanoclusters provide opportunities to conduct in-depth investigations. Devising well-defined nanocluster sensors based on fluorescence change is of particular interest not only for scientific studies but also for practical applications. Herein, the potential of the glutathionate (SG)-capped $Au_{25}$ nanocluster as a silver ion sensor is evaluated. The $Ag^+$ detection limit of approximately 200 nM, based on the fluorescence enhancement and good linear fluorescence response in the silver ion concentration range from 20 nM to 11 μM, in combination with the good selectivity among 20 types of metal cations, makes $Au_{25}(SG)_{18}$ a good candidate for fluorescent sensors for silver ions. Further experiments reveal three important factors responsible for the unique fluorescence enhancement caused by silver ions: 1) the oxidation state change of $Au_{25}(SG)_{18}$; 2) the interaction of neutral silver species ($Ag^0$, reduced by $Au_{25}(SG)_{18}^-$) with $Au_{25}(SG)_{18}$; and 3) the interaction of $Ag^+$ with $Au_{25}(SG)_{18}$. Experiments demonstrate the very different chemistry of hydrophobic $Au_{25}(SC_2H_4Ph)_{18}$ and hydrophilic $Au_{25}(SG)_{18}$ in the reaction with silver ions. This work indicates another potential application of gold nanoclusters, offers new strategies for nanocluster-based chemical sensing, and reveals a new way to influence nanocluster chemistry for potential applications.*

Prof. Z. Wu, M. Wang, J. Yang, Prof. W. Cai, Prof. G. Meng, H. Wang
Key Laboratory of Materials Physics
Anhui Key Laboratory of Nanomaterials and Nanostructures
Institute of Solid State Physics
Chinese Academy of Sciences, Hefei 230031, China
E-mail: zkwu@issp.ac.cn
Prof. X. Zheng
Key Laboratory of Materials Physics
Institute of Solid State Physics
Chinese Academy of Sciences, Hefei 230031, China
H. Qian, Prof. R. Jin
Department of Chemistry
Carnegie Mellon University
Pittsburgh, PA 15213, USA
E-mail: rongchao@andrew.cmu.edu

DOI: 10.1002/smll.201102590

## 1. Introduction

Gold nanoparticles comprising several to hundreds of atoms constitute a new class of material that is of major importance for both basic science studies and practical applications. Ultrasmall nanoparticles (<2 nm core diameter) are often called nanoclusters to differentiate them from their larger counterparts, plasmonic nanocrystals (typically >2 nm). Owing to the ultrasmall size, nanoclusters exhibit discrete electronic structure and distinctive properties that are fundamentally different from those of nanocrystals.[1] The latter generally possess a face-centered cubic (fcc) crystalline core and quasi-continuous electronic energy band structure.[1–4] Bulk solution-phase synthesis of atomically monodisperse nanoclusters has been achieved for a number of size-specific species protected by thiolates (referred to as $Au_n(SR)_m$, where $n$ is the number of gold atoms in the particle).


© 2012 Wiley-VCH Verlag GmbH & Co. KGaA, Weinheim

small NANO MICRO

Among the different-sized gold nanoclusters,[1,4–22] $Au_{25}$ has attracted much attention due to its interesting physicochemical properties[23–37] and potential applications in catalysis[38,39] and optics.[40,41] We have developed a size-focusing method for synthesizing highly pure $[Au_{25}(SR)_{18}]^-$ nanoclusters and a controlled oxidation route for converting $[Au_{25}(SR)_{18}]^-$ to $[Au_{25}(SR)_{18}]^0$.[42–44] The $Au_{25}(SR)_{18}$ structure was found to be independent of the surface ligands: we have proven that the same $Au_{25}$ core framework is retained regardless of the type of surface thiolate ligand (–SR = $SC_6H_{13}$ (*n*-hexanethiolate), $SC_{12}H_{25}$ (*n*-dodecanethiolate), and –SG (glutathione)).[25] The well-defined $Au_{25}(SR)_{18}$ clusters offer opportunities to correlate the properties with structure, which has led to an interesting finding that the ligands have significant influences on the fluorescence of the nanoclusters.[29] Among four types of thiolated $Au_{25}(SR)_{18}$ (where SR = $SC_6H_{13}$, $SC_{12}H_{25}$, $SC_2H_4Ph$ (phenylethylthiolate), and SG), glutathionate-capped $Au_{25}$ shows the strongest fluorescence at about 670 nm when excited at 514 nm.[29]

Fluorescent nanoparticles for ion detection are of great interest due to their simplicity and low detection limit (i.e., high sensitivity).[45] Although the fluorescence phenomena of gold nanoparticles have been known for a long time[26,40,46–53] (note that those nanoparticles with fluorescent ligands are not considered herein), their application to chemical sensing has been limited due primarily to the polydispersity of the particles and insufficient stability.[54] Huang et al. reported the detection of $Hg^{2+}$ by 11-mercaptoundecanoic acid (11-MUA)-protected gold nanoparticles (2.0 ± 0.1 nm) in the presence of 2,6-pyridinedicarboxylic acid (PDCA) based on an aggregation-induced quenching of fluorescence (AIQF).[54] Employing the same strategy, Muhammed et al. used bovine serum albumin (BSA)-protected gold nanoclusters to sense $Cu^{2+}$.[55] Chai et al. utilized another BSA-protected gold nanocluster to detect $Hg^{2+}$ at the 0.1 nM level.[56] The silver ion is less harmful than the mercury ion to living organisms; however, due to its wide employment in industry, such as electronics, photography, and pharmacy, a large amount of silver is being released into the environment annually from industrial wastes and emissions. Thus, it is of major importance to monitor the $Ag^+$ content levels in water systems. To the best of our knowledge, fluorescent gold nanoparticle-based sensors for silver ions have as yet been rarely reported.

The new class of nanocluster materials holds great promise for silver ion sensing. One obvious advantage of employing well-defined nanoclusters as sensors lies in that it can help understanding of the sensing mechanisms since in-depth investigations can be done, which will reveal insightful information for the changes (e.g., charge state, composition) of the nanocluster sensing material after interaction with ions. Another advantage lies in the fact that the materials may find more applications in other fields, such as biosensing and tracking, due to their ultrasmall size compared with larger nanoparticles (e.g., 10–100 nm). The fluorescent, stable, and atomically monodispersed $Au_{25}(SG)_{18}$ offers such a unique opportunity to devise a new type of nanosensor. Herein, we demonstrate the potential of $Au_{25}(SG)_{18}$ as a novel silver ion nanosensor. Interesting mechanisms and novel nanocluster chemistry have been revealed based upon detailed studies.

## 2. Results and Discussion

$Au_{25}(SG)_{18}$ was obtained as a black powder by using a previously reported method.[25,31,43] The UV/Vis–near infrared (NIR) and laser desorption ionization (LDI) mass spectra (see Figure S1, Supporting Information) confirm that the as-prepared nanoclusters are pure $Au_{25}(SG)_{18}$. The optical spectrum shows absorption peaks at approximately 670, 500, 445, 400, 320, and 280 nm that are characteristic of the $Au_{25}(SR)_{18}$ nanocluster.[31] LDI-MS shows the $Au_{25}S_{12}^-$ ion characteristic of $Au_{25}(SR)_{18}$; the loss of six sulfur atoms and all-G moieties is due to destructive LDI-MS.[25,31]

### 2.1. Sensitivity to $Ag^+$

$Au_{25}(SG)_{18}$ exhibits a maximum fluorescence emission at approximately 670 nm when excited at 514 nm (the shoulder at about 800 nm should be due to a sharp decay of the response of the photomultiplier tube (PMT) detector, see **Figure 1**a).[29] Interestingly, the addition of silver nitrate immediately causes large fluorescence enhancement (up to about 3 times). The fluorescence spectra of $Au_{25}(SG)_{18}$ with successive addition of silver ion are shown in Figure 1a. In a wide range of $Ag^+$ concentration from ≈20 nM to ≈22 μM, the emission monotonically increases with increasing $Ag^+$ concentration until a 3.4-fold fluorescence intensity (referenced to the initial fluorescence intensity in the absence of $Ag^+$) is obtained (see Figure 1a). The emission peak red-shifts with increasing silver ion concentration; after the addition of 24 μM silver nitrate, a ≈30 nm red-shift of the maximum emission is observed.

Further analysis reveals that there is a good linear relationship between the concentration of $Ag^+$ ranging from 20.2 nM to 11.1 μM and the fluorescence intensity (Figure 1b), which can be employed to detect $Ag^+$ in a quantitative manner in this concentration range. If the criterion of 10% fluorescence enhancement at 720 nm is employed to define the sensitivity of $Au_{25}(SG)_{28}$, then a detection limit of approximately 200 nM is achieved, which is much lower than the maximum allowable level (MAL) of $Ag^+$ ions (460 nM) in drinking water set up by the U.S. Environmental Protection Agency (EPA). For more quantitative evaluation of the $Au_{25}(SG)_{18}$ nanosensor, we tried some tap water samples. For uncontaminated tap water, $Au_{25}(SG)_{18}$ did not show a positive response; however, for contaminated (by $Ag^+$) tap water samples, it did indeed show obvious fluorescence enhancement, and the experimental results are in good agreement with those determined by inductively coupled plasma atomic emission spectroscopy (ICP-AES) analyses (parallel results by our method: 0.46, 0.49, 0.48 μM; ICP measurement: 0.52 μM; parallel results by our method: 2.31, 2.42, 2.50 μM; ICP measurement: 2.60 μM), thus indicating its good accuracy and precision for practical application.

 © 2012 Wiley-VCH Verlag GmbH & Co. KGaA, Weinheim 

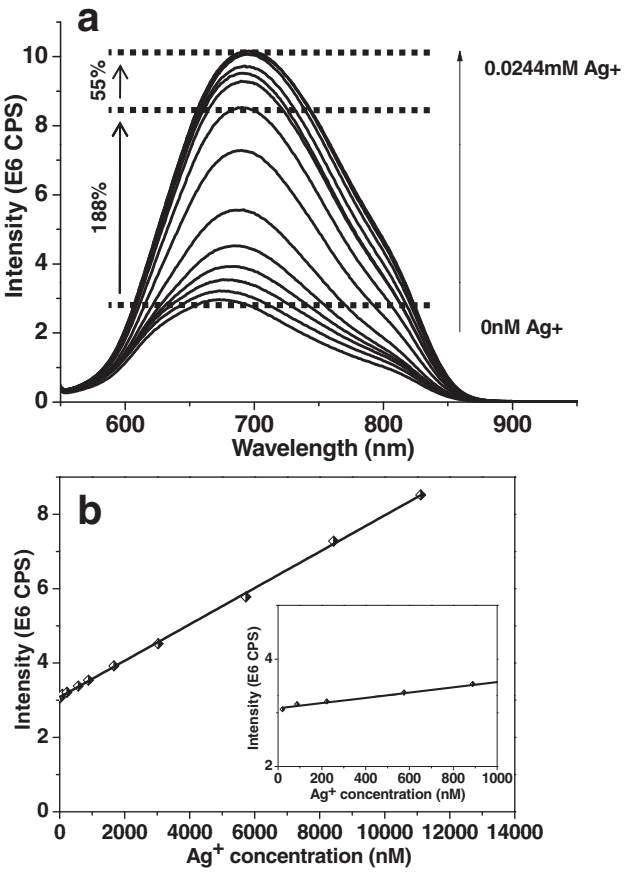


**Figure 1.** a) Fluorescence spectra of $Au_{25}(SG)_{18}$ (≈2.5 μM in $H_2O$) with successive titration of $Ag^+$ (0 nM, 86.5 nM, 888 nM, 1.67 μM, 3.03 μM, 5.73 μM, 8.43 μM, 11.1 μM, 13.8 μM, 16.4 μM, 19.1 μM, and 21.7 μM in the order of increasing amount). b) Linear relation between the $Ag^+$ concentration (20.2 nM–11.1 μM) and the fluorescence intensity. Inset: magnification of the linear relation in the concentration range from 20.2 to 1000 nM.

### 2.2. Selectivity to $Ag^+$

Interestingly, our further experiments found that 19 other types of metal ions ($Pb^{2+}$, $Cd^{2+}$, $Hg^{2+}$, $Cu^{2+}$, $Zn^{2+}$, $Ni^{2+}$, $Co^{3+}$, $Tb^{3+}$, $Eu^{3+}$, $Pd^{2+}$, $Fe^{2+}$, $Fe^{3+}$, $Mg^{2+}$, $K^+$, $Na^+$, $Ca^{2+}$, $Cr^{3+}$, $Mn^{2+}$, $Au^{3+}$) did indeed cause partial quenching of fluorescence of $Au_{25}(SG)_{18}$ over a large concentration range from about $10^{-7}$ M to about $10^{-3}$ M (as opposed to fluorescence enhancement in the case of $Ag^+$); see **Figure 2** (for $Pd^{2+}$) and Figures S2–S19 in the Supporting Information (for other ions). Figure S20 shows an intuitive comparison. These ions quench the $Au_{25}$ fluorescence to a different extent. For example, a few types of ions quench the fluorescence dramatically, such as $Co^{2+}$, in which a 40 nM concentration results in a 36% fluorescence decrease (see Figure S10). Some types of ions quench the fluorescence moderately; one example is $Au^{3+}$: ≈1.9 mmol $Au^{3+}$ causes only 11% fluorescence intensity decrease (see Figure S11). With the addition of metal ions, the maximum emission at 670 nm gradually shifts to ≈700 nm mainly due to complexation (for silver and a few other cations, the oxidation cannot be neglected, see discussion below). Notice that,

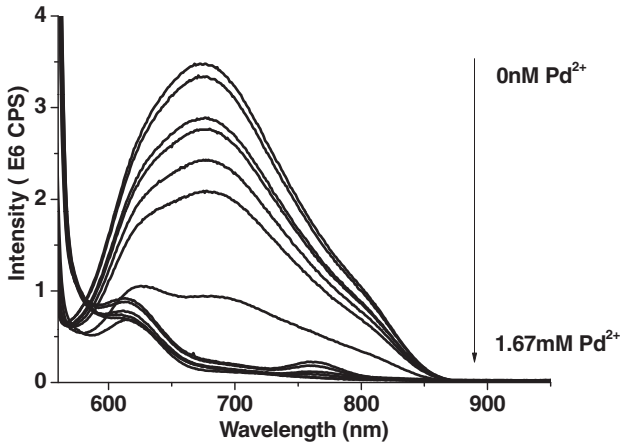


**Figure 2.** Fluorescence quenching of $Au_{25}(SG)_{18}$ with successive titration of $Pd^{2+}$ (0 nM, 84.6 nM, 478 nM, 1.16 μM, 2.20 μM, 6.89 μM, 35.0 μM, 85.8 μM, 163 μM, 414 μM, 1.12 mM, and 1.67 mM in the order of increasing amount).

with the decrease in $Au_{25}(SG)_{18}$ emission, the background peak coming from the solvent (water) at ≈620 nm becomes prominent.

### 2.3. Oxidation- and Interaction-Induced Fluorescence Enhancement

The fluorescence quenching could be due to the heavy atom's effect and/or aggregation of $Au_{25}(SG)_{18}$ after being complexed with metal cations, as other researchers have reported (our observation of precipitates after concentrating the solutions provides direct and obvious evidence; note that under the same conditions, sole $Au_{25}(SG)_{18}$ without the coexistence of metal ions does *not* precipitate).[54–56] A slight enhancement of fluorescence would not be of significant importance; however, the 3.4-fold fluorescence enhancement is worthy of an in-depth investigation. To understand the unique performance of $Ag^+$, several possibilities should be considered: 1) silver ions form some fluorescent Ag–SG complexes; 2) silver ions themselves form fluorescent species when reduced by $Au_{25}(SG)_{18}$; 3) oxidation of $Au_{25}(SG)_{18}$ results in enhancement of its own fluorescence; 4) silver ions interact with $Au_{25}(SG)_{18}$ (or the highly charged $Au_{25}(SG)_{18}$) and cause the fluorescence enhancement (with the composition of $Au_{25}(SG)_{18}$ unchanged); 5) reduced silver species interact with $Au_{25}(SG)_{18}$ (or the highly charged $Au_{25}(SG)_{18}$) and lead to the fluorescence enhancement (without changing the composition of $Au_{25}(SG)_{18}$); and 6) replacement of Au site(s) in $Au_{25}$ by Ag atom(s) results in the emission enhancement (i.e., the composition of $Au_{25}(SG)_{18}$ undergoes some change and bimetal nanoclusters may be formed). Below we consider all the above possibilities one by one.

The fact that the mixture of $AgNO_3$ and glutathione shows negligible luminescence excludes the first possibility. Also, addition of a reducing reagent such as $NaBH_4$ or ascorbic acid to the above mixture does not cause any obvious fluorescence change, which excludes the second possibility. Oxidation of $Au_{25}(SG)_{18}$ by $H_2O_2$ does lead to significant

 © 2012 Wiley-VCH Verlag GmbH & Co. KGaA, Weinheim 

small NANO MICRO

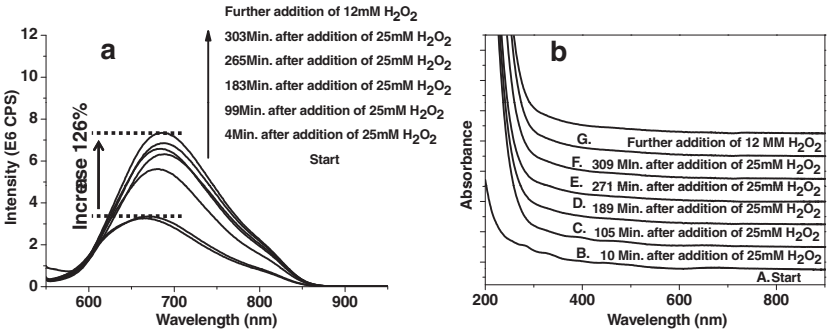


**Figure 3.** Oxidation process of $Au_{25}(SG)_{18}$ monitored by a) fluorescence and b) UV/Vis–NIR absorption spectroscopy (for the overlaid view, see Figure S39 in the Supporting Information).

enhancement of emission (see **Figure 3**a), thus indicating that the third possibility perhaps exists. The oxidation of $Au_{25}$ by $H_2O_2$ is a slow process, which is reflected in the gradual, time-dependent increase of fluorescence. In our case, about 4 h after the addition of 25 mM $H_2O_2$, the fluorescence intensity increased to the maximum, nearly 2.3-fold compared with the initial intensity. Of note, the addition of more excessive $H_2O_2$ can accelerate the oxidation process, but it does not change the maximum emission intensity in some concentration ranges, which implies that the maximum emission relates to certain charge state(s) of $Au_{25}$. It is known that $Au_{25}$ has multiple charge states and each charge state shows a distinct UV/Vis–NIR spectrum;[29,32,33,44,57,58] Figure 3b (also see Figure S39) shows the time dependence of $Au_{25}(SG)_{18}$ optical absorption after 25 mM $H_2O_2$ was reached. About 4 h later the UV/Vis–NIR spectra became stable. No further change was observed after adding more $H_2O_2$ and an even further prolonged time, which implies the formation of the highest charged $Au_{25}$ (tentatively assigned $[Au_{25}]^{2+}$); note that mass spectrometry characterization confirmed the $Au_{25}$ formula, though its charge states could not be confirmed.[29] A similar oxidation process occurs when $Ag^+$ is added to an $Au_{25}(SG)_{18}$ solution (see **Figure 4**). The isosbestic points at 394, 462, and 612 nm indicate a stoichiometric redox reaction between $Ag^+$ and $Au_{25}(SG)_{18}$; the completion of oxidation takes totally about 3 equiv $Ag^+$, consistent with the $Au_{25}$ charge transfer from –1 to +2. X-ray photoelectron spectroscopy (XPS) analyses provide other, more direct evidence for the oxidation of $Au_{25}(SG)_{18}$ by $Ag^+$ (see Figure S40): a positive 0.15 eV shift (to higher energy) was observed for the binding energy of Au4f after $Au_{25}(SG)_{18}$ reacted with 2.8 equiv $Ag^+$.

One question is why stronger oxidizing ions such as $Au^{3+}$ and $Hg^{2+}$ do not cause the fluorescence enhancement in $Au_{25}(SG)_{18}$ as the silver ion does. The reason is probably the strong fluorescence quenching effect of such heavy ions or their chemically reduced species. This prompted us to investigate the effect of the silver ion itself on the fluorescence of $Au_{25}(SG)_{18}$. It was found that addition of adequate $Ag^+$ led to further enhancement of emission of $Au_{25}(SG)_{18}$ after the completion of oxidation by $H_2O_2$ or $Ag^+$ (see Figure 1 and **Figure 5**). In both cases (case 1: oxidizing $Au_{25}$ by $Ag^+$, then further adding $Ag^+$, see Figure 1; case 2: oxidizing $Au_{25}$ by $H_2O_2$, then adding $Ag^+$, see Figure 5a), the post-oxidation processes have some similarities reflected in the fluorescence change: 1) the maximum fluorescence increase amplitudes, expressed as $(I_{max}–I_0)/I_{max}$, where $I_0$ is the fluorescence intensity without further addition of silver ions and $I_{max}$ is the maximum fluorescence intensity after further addition of silver ions, are comparable (55.3 and 60.0%, respectively); 2) the fluorescence intensity has somehow a linear relationship with the silver ion concentration in a certain range and even the linear regression coefficients are rather close ($1.75 \times 10^{-4}$ and $1.66 \times 10^{-4}$, respectively, see Figure 5b); and 3) the amounts of silver ions needed to stimulate the strongest emission after the completion of $Au_{25}(SG)_{18}$ oxidation are both about 5 equivalents (relative to $Au_{25}$), which suggests that the strongest fluorescence relates to a certain structured complex. Such similarities in the two cases confirm that the silver ions themselves can contribute to the fluorescence enhancement in $Au_{25}(SG)_{18}$, probably due to a chelation-enhanced fluorescence (CHEF) mechanism.[59–61] The red-shift of emission in both cases with the silver addition after the completion of oxidation also indicates the complexation of $Au_{25}$ with silver cations.

We now consider the effect of the reduced silver species (neutral silver, $Ag^0$, from the stoichiometric redox reaction between $Ag^+$ and $Au_{25}(SG)_{18}$) on the fluorescence of $Au_{25}(SG)_{18}$. In the above two cases, the post-oxidation processes are similar; however, a difference is still found in the amplitude of fluorescence increase during the oxidation process. In the first case (oxidized directly by $Ag^+$), the fluorescence increase amplitude is 188%, in contrast with the 126% increase in amplitude in the second case (oxidized by $H_2O_2$). The gap cannot be simply attributed to the slightly excess $Ag^+$ since about 5 equiv $Ag^+$ only causes an ≈60% intensity increase. There is no other suspected species except the reduced Ag (mainly $Ag^0$) in the redox process, and the probable reason could

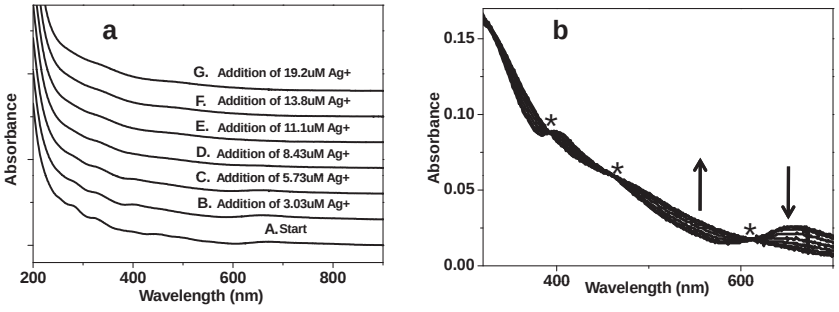


**Figure 4.** a) UV/Vis–NIR spectra of $Au_{25}(SG)_{18}$ (≈2.5 μM in $H_2O$) with successive titration of $Ag^+$. b) An overlaid view, with the isosbestic points at 394, 462, and 612 nm marked by asterisks; the arrows show the trends of changes in absorption.


© 2012 Wiley-VCH Verlag GmbH & Co. KGaA, Weinheim

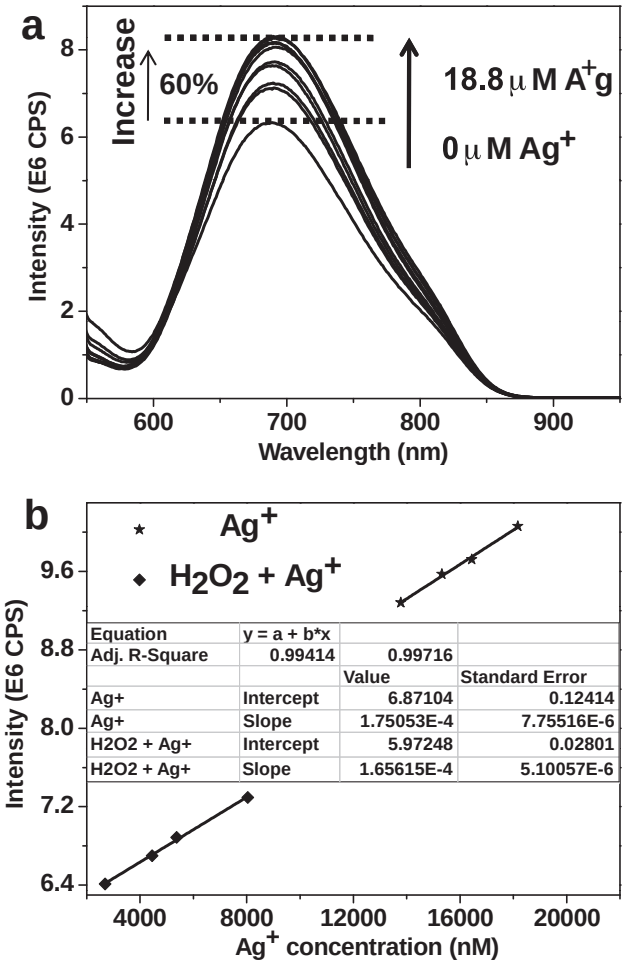


Figure 5. a) Fluorescence spectra of $Au_{25}(SG)_{18}$ with further successive titration of $Ag^+$ after the completion of oxidation (0, 1.34, 2.69, 4.45, 5.37, 8.04, 10.7, 13.4, 16.1, and 18.8 μM in the order of increasing amount). b) Fluorescence intensity change with further addition of $Ag^+$ after the completion of oxidation of $Au_{25}(SG)_{18}$ by $Ag^+$ (top) and $H_2O_2$ (bottom); inset: fitting results.

be the interaction between $Ag^0$ and oxidized $Au_{25}$, which is similar to a metal-enhanced fluorescence (MEF) effect.[62–67] However, the XPS analyses did not detect the neutral silver species (see below), which may be due to the instability of neutral silver species without protection or other unknown reason.

For the fluorescence enhancement mechanism, another possibility is that silver atoms replace the gold sites in $Au_{25}$, forming stable bimetal nanocluster $Au_{25-x}Ag_x(SG)_{18}$. Previous work demonstrated that, in the case of phenylethylthiolated $Au_{25}(SC_2H_4Ph)_{18}$, this kind of replacement can indeed occur between the $Au_{25}(SC_2H_4Ph)_{18}$ and $Ag^+$, evidenced by mass spectrometric analysis.[68] We also investigated interaction of $Ag^+$ with phenylethylthiolated $Au_{25}(SC_2H_4Ph)_{18}$; as shown in Figure S41, $Au_{24}AgS_{12}^-$, $Au_{23}Ag_2S_{12}^-$, and $Au_{22}Ag_3S_{12}^-$, instead of $Au_{25}S_{12}^-$, were found to sequentially dominate the mass spectra, thereby indicating the formation of the main species $Au_{24}Ag(SC_2H_4Ph)_{18}$, $Au_{23}Ag_2(SC_2H_4Ph)_{18}$, and $Au_{22}Ag_3(SC_2H_4Ph)_{18}$ with increasing equivalents of silver ion. For $Au_{25}(SG)_{18}$ after treatment with $Ag^+$, reliable mass spectra related to the intact cluster ion or the main fragments (typically $Au_{25}S_{12}^-$) are unfortunately difficult to obtain; thus, as an alternative, XPS analyses were conducted. To do this, five samples were made.

In a typical experiment, $Au_{25}$ was mixed with 2.9 equiv $Ag^+$, then excess MeOH was added, resulting in precipitation; the collected solid was washed thoroughly by MeOH, dried, and named sample (1). Samples (2) and (3) were made by the same protocol but with adjustment of the amount of silver to 9.0 and 30.0 equiv, respectively. Sample (4) was made by the following protocol: after glutathione (GSH) was mixed with 6.0 equiv $Ag^+$, excess MeOH was added, then the precipitate was collected, washed thoroughly by MeOH, and dried. For sample (5), $Au_{25}$ was first oxidized with excess $H_2O_2$ (ca. 1000 equiv; the process can be monitored by UV/Vis–NIR spectroscopy), subsequently 11.5 equiv $Ag^+$ was introduced, and then excess MeOH was added; the collected solid was washed thoroughly by MeOH, dried, and designated as sample (5), which serves as a reference of silver(I) analogue owing to the complete oxidation of $Au_{25}$ by excess $H_2O_2$ and no redox reaction happens between $Au_{25}$ and $Ag^+$. The XPS results (**Figure 6**) show similar featured signals of silver(I) for samples (1), (2), (3), and (5), which indicates that there may be no neutral silver in these samples. However, the XPS analyses of the reaction product of $Au_{25}(SC_2H_4Ph)_{18}$ with

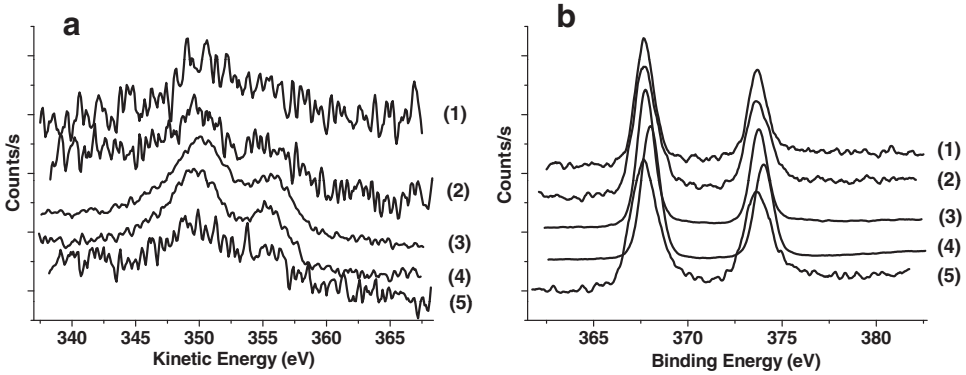


Figure 6. XPS of treated $Au_{25}(SG)_{18}$ compared with Ag–SG complex; a) AgMN1 scan; b) Ag3d scan. The graphs are vertically shifted and enlarged for convenience of comparison. Note: 1) $Au_{25}(SG)_{18}$ reacted with 2.9 equiv $Ag^+$; 2) $Au_{25}(SG)_{18}$ reacted with 9.0 equiv $Ag^+$; 3) $Au_{25}(SG)_{18}$ reacted with 30.0 equiv $Ag^+$; 4) $Ag^+$ reacted with 6.0 equiv GSH; 5) $Au_{25}$ was mixed with 11.5 equiv $Ag^+$ after oxidation by enough $H_2O_2$; for details, see the text.


© 2012 Wiley-VCH Verlag GmbH & Co. KGaA, Weinheim

NANO MICRO small

$Ag^+$ show that the Ag3d binding energy obviously shifts to a higher energy; a 0.55 eV shift in $Ag3d_{5/2}$ binding energy was observed, in comparison with no obvious shift in $Ag3d_{5/2}$ for the reaction product of $Au_{25}(SG)_{18}$ with $Ag^+$. In the case of the reaction product of $Au_{25}(SC_2H_4Ph)_{18}$ with $Ag^+$, the Ag3d binding energy matches that of pure silver very well ($Ag3d_{5/2}$ and $Ag3d_{3/2}$ of pure silver: 368.2 and 374.2 eV, respectively; measured $Ag3d_{5/2}$ and $Ag3d_{3/2}$ of $Au_{25}(SC_2H_4Ph)_{18}$/Ag system: average 368.2 and 374.2 eV, respectively; see Figure S42). Thus, our conclusion is that silver/gold atom exchange occurred in the phenylethylthiolate-protected cluster, forming $Au_{25-x}Ag_x(SC_2H_4Ph)_{18}$, but such an exchange process does not occur to $Au_{25}(SG)_{18}$.

The above conclusion is also supported by other evidence. UV/Vis–NIR absorption shows an obvious difference between the two systems (**Figure** 4 and **7**). With the addition of silver ions, the characteristic absorption peaks of $Au_{25}(SC_2H_4Ph)_{18}$ (such as the peaks at 395, 445, and 680 nm) change more slowly than in the case of $Au_{25}(SG)_{18}$ under comparable conditions. For a detailed comparison, see Figure 7b. The Au/S atom ratios determined by XPS for various samples (Table S1, Supporting Information) also support the notion that Au is not replaced by Ag in the $Au_{25}(SG)_{18}$ system, because the determined Au/S atom ratio (1.40 ± 0.04) for all the $Au_{25}(SG)_{18}$ samples after interaction with various amounts of $Ag^+$ agrees well with the Au/S atom ratio of pristine $Au_{25}(SG)_{18}$ (theoretical Au/S: 25/18 = 1.39, measured Au/S = 1.40, see Table S1). Furthermore, the very low concentration of gold ions detected in the remaining solution after $Au_{25}(SG)_{18}$ reacts with excess silver(I) (e.g., 30 equiv $Ag^+$) can provide further proof. The reason is that, if the replacement took place, $Au_{25}(SG)_{18}$ could react with at least 1 equiv $Ag^+$ and form $Au_{24}Ag(SG)_{18}$; then the expected gold ion concentration (released due to silver displacement) in the solution in our case should be at least 10.0 ppm (the more replaced, the higher the Au ion concentration). But our experiment shows that actually the gold ion concentration is only 0.090 ppm, which is negligible. Taken together, our results confirm that Ag does not replace Au in $Au_{25}(SG)_{18}$, although it does in the $Au_{25}(SCH_2CH_2Ph)_{18}$ system.

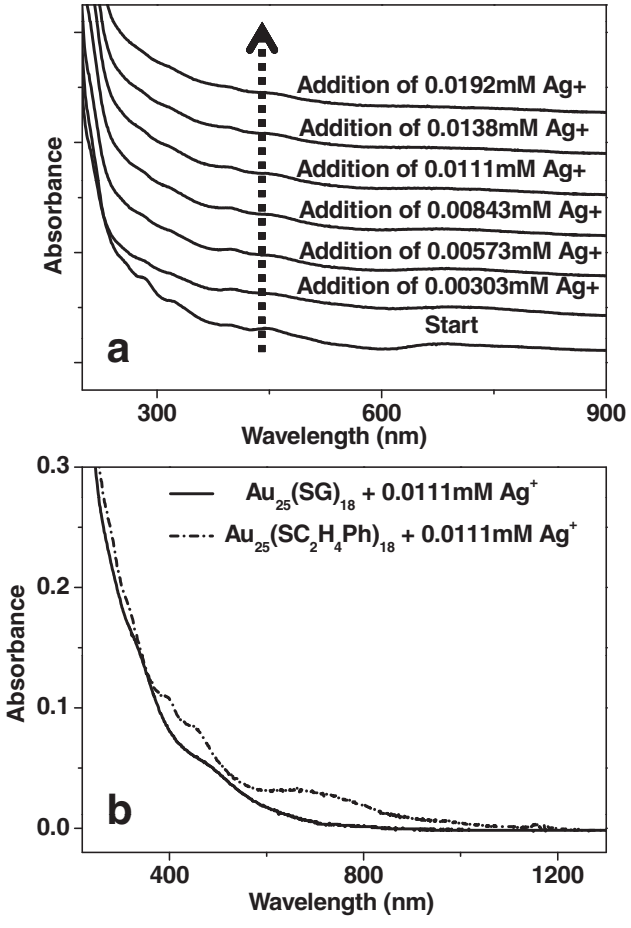


**Figure 7.** a) UV/Vis–NIR spectra of $Au_{25}(SC_2H_4Ph)_{18}$ (≈2.5 μM in $CH_3CN$) with successive titration of $Ag^+$. b) Comparison of the UV/Vis–NIR absorption spectra of two kinds of $Au_{25}$ with different ligands ($Au_{25}(SC_2H_4Ph)_{18}$, $Au_{25}(SG)_{18}$) after the addition of 11.1 μM $Ag^+$.

The difference in the reaction pathways between $Au_{25}(SG)_{18}$ and $Au_{25}(SC_2H_4Ph)_{18}$ with $Ag^+$ is probably due to the ligands: the strong coordination of –SG with silver ions is believed to prevent the replacement between $Ag^+$ and $Au^0$ in $Au_{25}(SG)_{18}$, whereas the $Au_{25}(SC_2H_4Ph)_{18}$ cluster would be readily attacked by $Ag^+$ since the $SC_2H_4Ph$ ligand has no functional group that can coordinate with $Ag^+$.

In all, three processes are identified that contribute to the fluorescence enhancement: the first is the oxidation of $[Au_{25}(SG)_{18}]^-$ to higher oxidation states; the second is the interaction of $Ag^+$ with $Au_{25}(SG)_{18}$; and the last is the interaction of $Ag^0$ species with $Au_{25}$. As to the replacement of $Ag^+$ with $Au^0$, it occurs to the $Au_{25}(SC_2H_4Ph)_{18}$ cluster but no evidence was found in the case of $Au_{25}(SG)_{18}$.

The mechanisms involved for emission in nanoparticles affect their functions and further applications. Herein, we briefly discuss several proposed models. A theoretical study explained the fluorescence of noble-metal nanoparticles by electronic transitions between the occupied d band and states above the Fermi level (usually the sp band).[69] Murray et al. attributed the fluorescence to transitions between the $5d^{10}$ band and the $6(sp)^1$ band.[27] Other possible mechanisms have been suggested, such as ligand-to-metal charge transfer[54] and ligand-to-metal–metal charge transfer.[70] For $Au_{25}(SG)_{18}$, the mechanism is rather complicated.[29] The excitation spectrum is obviously different from the absorption spectrum (see Figure S43); both the maximum emission wavelength and the emission intensity are influenced by the excitation energy (i.e., excited wavelength) in the selected range ($\lambda$: 450–600 nm), especially when the excited energy is less than ≈2.4 eV ($\lambda > 514$ nm, see Figure S44). Given that the valence electrons have a large influence on the fluorescence intensity, we attribute the sp–sp intraband transition as being the main source of the observed fluorescence, which is also consistent with previous theoretical calculations.[71,72]

## 3. Conclusion

A novel type of nanosensor utilizing well-defined gold nanoclusters has been developed. Based on the fluorescence enhancement, the potential of $Au_{25}(SG)_{18}$ as a silver sensor

 © 2012 Wiley-VCH Verlag GmbH & Co. KGaA, Weinheim 

has been evaluated in detail. The experimental results demonstrate that $Au_{25}(SG)_{18}$ can be a potential silver ion nanosensor with a detection limit of approximately 200 nM and good selectivity against other cations ($Pd^{2+}$, $Cd^{2+}$, $Hg^{2+}$, $Cu^{2+}$, $Zn^{2+}$, $Ni^{2+}$, $Co^{3+}$, $Tb^{3+}$, $Eu^{3+}$, $Pb^{2+}$, $Fe^{2+}$, $Fe^{3+}$, $Mg^{2+}$, $K^{+}$, $Na^{+}$, $Ca^{2+}$, $Cr^{3+}$, $Mn^{2+}$, $Au^{3+}$). Furthermore, three factors are found to be primarily responsible for the unique fluorescence enhancement in $Au_{25}(SG)_{18}$ when sensing $Ag^{+}$ ions. Among them, the oxidation (leading to a higher charge state of $Au_{25}$) contributes most (causing a ca. 126% increase in fluorescence intensity), with the other two contributions coming from the interactions of $Ag^{+}$ with $Au_{25}$ (leading to a ca. 55% increase in fluorescence intensity) and $Ag^{0}$ with $Au_{25}$ (giving a ca. 62% increase of fluorescence intensity). These interesting discoveries can be employed as novel strategies (different from AIQF) for nanocluster-based chemical sensing. Another interesting finding is that the ligands have different influences on the replacement between $Ag^{+}$ and $Au^{0}$ in $Au_{25}$. The replacement can readily occur between the phenylethylthiolated $Au_{25}(SC_2H_4Ph)_{18}$ and $Ag^{+}$, but it is prevented in glutathionate-capped $Au_{25}(SG)_{18}$; the latter is attributed to the strong coordination of the ligands with the silver ion. Overall, our work offers important insights into the nanocluster fluorescence and chemical properties, which may facilitate potential application of nanocluster materials to chemical sensing.

## 4. Experimental Section

*Chemicals*: Hydrogen tetrachloroaurate hydrate ($HAuCl_4 \cdot 3H_2O$, ≥99.9%, Shanghai Chemical Reagent Co., Ltd), L-glutathione (GSH, $C_{10}H_{17}N_3O_6S$, ≥99%, Aldrich), and hydrogen peroxide ($H_2O_2$, 30%, Suzhou Chemical Reagent Co., Ltd) were obtained as indicated. For other chemicals' details, see the Supporting Information. All chemicals were used as received. Nanopure water (resistivity 18.2 MΩ cm) was produced with a Barnstead NANO pure water system.

*Characterization*: All UV/Vis–NIR absorption spectra were recorded in the range of 200–1400 nm using a UV3600 spectrophotometer. Laser desorption/ionization (i.e., no matrix, LDI) mass spectrometry analyses were performed with a PerSeptive Biosystems Voyager DE super-STR time-of-flight (TOF) mass spectrometer. Fluorescence spectra were recorded on a Fluoromax-4 spectrofluorometer (HORIBA Jobin Yvon). XPS measurements were performed on a Thermo ESCALAB 250 instrument configured with a monochromated $Al_{K\alpha}$ (1486.8 eV) 150 W X-ray source, 0.5 mm circular spot size, a flood gun to counter charging effects, and the analysis chamber base pressure $<1 \times 10^{-9}$ mbar; data were collected with FAT = 20 eV. The takeoff angle, defined as the angle between the substrate normal and the detector, was fixed at 0°. Substrates were mounted on standard sample studs by means of double-sided adhesive tape. All binding energies were calibrated using either the $Au4f_{7/2}$ peak (84.0 eV) or the C1s carbon peak (284.6 eV). ICP-AES (ICP6000, Thermal Electron) was used to measure the concentration of ions.

*Synthesis of $Au_{25}(SR)_{18}$ Clusters*: The $Au_{25}(SG)_{18}$ nanoclusters were synthesized by following a reported method.[25,29,43]

*Titration*: The titrations of various ions were conducted in a quartz cuvette (1 cm beam path). Briefly, small amounts (typically several microliters) of concentrated salt solutions were added to a 2.5 μM $Au_{25}(SG)_{18}$ aqueous solution, and the final concentrations of cations were adjusted by the volume of $Au_{25}(SR)_{18}$ solution (initially fixed at 2.5 mL).

## Supporting Information

*Supporting Information is available from the Wiley Online Library or from the author.*

## Acknowledgements

*Z.W. acknowledges the Hundred Talent Program of the Chinese Academy of Sciences, National Basic Research Program of China (#2007CB936604), and the Natural Science Foundation of China (Grant no. 21171170). R.J. is grateful for the support by AFOSR.*

[1] R. Jin, *Nanoscale* **2010**, *2*, 343–362.
[2] Z. Wu, J. Chen, R. Jin, *Adv. Funct. Mater.* **2011**, *21*, 177–183.
[3] J. P. Wilcoxon, B. L. Abrams, *Chem. Soc. Rev.* **2006**, *35*, 1162–1194.
[4] J. F. Parker, C. A. Fields-Zinna, R. W. Murray, *Acc. Chem. Res.* **2010**, *43*, 1289–1296.
[5] T. G. Schaaff, M. N. Shafigullin, J. T. Khoury, I. Vezmar, R. L. Whetten, W. G. Cullen, P. N. First, C. Gutierrez-Wing, J. Ascensio, M. J. Jose-Yacaman, *J. Phys. Chem. B.* **1997**, *101*, 7885–7891.
[6] T. G. Schaaff, G. Knight, M. N. Shafigullin, R. F. Borkman, R. L. Whetten, *J. Phys. Chem. B* **1998**, *102*, 10643–10646.
[7] M. J. Hostetler, J. E. Wingate, C.-J. Zhong, J. E. Harris, R. W. Vachet, M. R. Clark, J. D. Londono, S. J. Green, J. J. Stokes, G. D. Wignall, G. L. Glish, M. D. Porter, N. D. Evans, R. W. Murray, *Langmuir* **1998**, *14*, 17–30.
[8] R. L. Donkers, D. Lee, R. W. Murray, *Langmuir* **2004**, *20*, 1945–1952.
[9] M. W. Heaven, A. Dass, P. S. White, K. M. Holt, R. W. Murray, *J. Am. Chem. Soc.* **2008**, *130*, 3754–3755.
[10] Y. Negishi, K. Nobusada, T. Tsukuda, *J. Am. Chem. Soc.* **2005**, *127*, 5261–5270.
[11] N. K. Chaki, Y. Negishi, H. Tsunoyama, Y. Shichibu, T. Tsukuda, *J. Am. Chem. Soc.* **2008**, *130*, 8608–8610.
[12] Z. Wu, M. A. MacDonald, J. Chen, P. Zhang, R. Jin, *J. Am. Chem. Soc.* **2011**, *133*, 9670–9673.
[13] E. S. Shibu, M. A. H. Muhammed, T. Tsukuda, T. Pradeep, *J. Phys. Chem. C* **2008**, *112*, 12168–12176.
[14] E. S. Shibu, T. Pradeep, *Chem. Mater.* **2011**, *23*, 989–999.
[15] Y. Levi-Kalisman, P. D. Jadzinsky, N. Kalisman, H. Tsunoyama, T. Tsukuda, D. A. Bushnell, R. D. Kornberg, *J. Am. Chem. Soc.* **2011**, *133*, 2976–2982.
[16] G. H. Woehrle, M. G. Warner, J. E. Hutchison, *J. Phys. Chem. B.* **2002**, *106*, 9979–9981.
[17] A. P. Gies, D. M. Hercules, A. E. Gerdon, D. E. Cliffel, *J. Am. Chem. Soc.* **2007**, *129*, 1095–1104.
[18] O. Toikkanen, V. Ruiz, G. R nnholm, N. Kalkkinen, P. Liljeroth, B. M. Quinn, *J. Am. Chem. Soc.* **2008**, *130*, 11049–11055.
[19] A. Dass, *J. Am. Chem. Soc.* **2009**, *131*, 11666–11667.
[20] J. Zheng, J. T. Petty, R. M. Dickson, *J. Am. Chem. Soc.* **2003**, *125*, 7780–7781.
[21] Z. Tang, B. Xu, B. Wu, M. W. Germann, G. Wang, *J. Am. Chem. Soc.* **2010**, *132*, 3367–3374.

 © 2012 Wiley-VCH Verlag GmbH & Co. KGaA, Weinheim 

[22] J. M. Pettibone, J. W. Hudgens, *ACS Nano* **2011**, *5*, 2989–3002.
[23] Y. Negishi, H. Tsunoyama, M. Suzuki, N. Kawamura, M. M. Matsushita, K. Maruyama, T. Sugawara, T. Yokoyama, T. Tsukuda, *J. Am. Chem. Soc.* **2006**, *128*, 12034–12035.
[24] T. G. Schaaff, R. L. Whetten, *J. Phys. Chem. B* **2000**, *104*, 2630–2641.
[25] Z. Wu, C. Gayathri, R. R. Gil, R. Jin, *J. Am. Chem. Soc.* **2009**, *131*, 6535–6542.
[26] S. Link, A. Beeby, S. FitzGerald, M. A. El-Sayed, T. G. Schaaff, R. L. Whetten, *J. Phys. Chem. B* **2002**, *106*, 3410–3415.
[27] G. Wang, T. Huang, R. W. Murray, L. Menard, R. G. Nuzzo, *J. Am. Chem. Soc.* **2005**, *127*, 812–813.
[28] M. S. Devadas, J. Kim, E. Sinn, D. Lee, T. Goodson III, G. Ramakrishna, *J. Phys. Chem. C* **2010**, *114*, 22417–22423.
[29] Z. Wu, R. Jin, *Nano Lett.* **2010**, *10*, 2568–2573.
[30] R. Hamouda, B. Bellina, F. Bertorelle, I. Compagnon, R. Antoine, M. Broyer, D. Rayane, P. Dugourd, *J. Phys. Chem. Lett.* **2010**, *1*, 3189–3194.
[31] Z. Wu, R. Jin, *ACS Nano* **2009**, *3*, 2036–2042.
[32] R. Guo, R. W. Murray, *J. Am. Chem. Soc.* **2005**, *127*, 12140–12143.
[33] Y. Negishi, N. K. Chaki, Y. Shichibu, R. L.Whetten, T. Tsukuda, *J. Am. Chem. Soc.* **2007**, *129*, 11322–11323.
[34] D. G. Georganopoulou, M. V. Mirkin, R. W. Murray, *Nano Lett.* **2004**, *4*, 1763–1767.
[35] W. Chen, S. W. Chen, *Angew. Chem.* **2009**, *121*, 4450–4453; *Angew. Chem. Int. Ed.* **2009**, *48*, 4386–4389.
[36] S. Antonello, A. H. Holm, E. Instuli, F. Maran, *J. Am. Chem. Soc.* **2007**, *129*, 9836–9837.
[37] D. Garca-Raya, R. Madueo, M. Blzquez, T. Pineda, *J. Phys. Chem. C* **2009**, *113*, 8756–8761.
[38] Y. Zhu, H. Qian, B. A. Drake, R. Jin, *Angew. Chem.* **2010**, *122*, 1317–1320;*Angew. Chem. Int. Ed.* **2010**, *49*, 1295–1298.
[39] Y. Liu, H. Tsunoyama, T. Akita, T. Tsukuda, *Chem. Commun.* **2010**, *46*, 550–552.
[40] G. Ramakrishna, O. Varnavski, J. Kim, D. Lee, T. Goodson, *J. Am. Chem. Soc.* **2008**, *130*, 5032–5033.
[41] M. A. H. Muhammed, A. K. Shaw, S. K. Pal, T. Pradeep, *J. Phys. Chem. C* **2008**, *112*, 14324–14330.
[42] M. Zhu, E. Lanni, N. Garg, M. E. Bier, R. Jin, *J. Am. Chem. Soc.* **2008**, *130*, 1138–1139.
[43] Z. Wu, J. Suhan, R. Jin, *J. Mater. Chem.* **2009**, *19*, 622–626.
[44] M. Zhu, W. T. Eckenhoff, T. Pintauer, R. Jin, *J. Phys. Chem. C* **2008**, *112*, 14221–14224.
[45] G. Aragay, J. Pons, A. Merkoçi, *Chem. Rev.* **2011**, *111*, 3433–3458.
[46] C. Zhou, C. Sun, M. Yu, Y. Qin, J. Wang, M. Kim, J. Zheng, *J. Phys. Chem. C* **2010**, *114*, 7727–7732.
[47] X. Huang, X. Zhou, S. Wu, Y. Wei, X. Qi, J. Zhang, F. Boey, H. Zhang, *Small* **2010**, *6*, 513–516.
[48] R. J. Zhou, M. M. Shi, X. Q. Chen, M. Wang, H. Z. Chen, *Chem. Eur. J.* **2009**, *15*, 4944–4951.
[49] X. Liu, C. Li, J. Xu, J. Lv, M. Zhu, Y. Guo, S. Cui, H. Liu, S. Wang, Y. Li, *J. Phys. Chem. C* **2008**, *112*, 10778–10783.
[50] Y. Bao, C. Zhong, D. M. Vu, J. P. Temirov, R. B. Dyer, J. S. Martinez, *J. Phys. Chem. C* **2007**, *111*, 12194–12198.
[51] M. Sakamoto, T. Tachikawa, M. Fujitsuka, T. Majima, *J. Am. Chem. Soc.* **2009**, *131*, 6–7.
[52] K.-M. Lam, P.-H. Chan, K.-Y. Wong, *J. Nanosci. Nanotechnol.* **2009**, *9*, 2337–2345.
[53] D. Lee, R. L. Donkers, G. Wang, A. S. Harper, R. W. Murray, *J. Am. Chem. Soc.* **2004**, *126*, 6193–6199.
[54] C.-C. Huang, Z. Yang, K.-H. Lee, H.-T. Chang, *Angew. Chem.* **2007**, *119*, 6948–6952; *Angew. Chem. Int. Ed.* **2007**, *46*, 6824–6828.
[55] M. A. H. Muhammed, P. K. Verma, S. K. Pal, A. Retnakumari, M. Koyakutty, S. Nair, T. Pradeep, *Chem. Eur. J.* **2010**, *16*, 10103–10112.
[56] F. Chai, T. Wang, L. Li, H. Liu, L. Zhang, Z. Su, C. Wang, *Nanoscale Res. Lett.* **2010**, *5*, 1856–1860.
[57] A. Venzo, S. Antonello, J. A. Gascon, I. Guryanov, R. D. Leapman, N. V. Perera, A. A. Sousa, M. Zamuner, A. Zanella, F. Maran, *Anal. Chem.* **2011**, *83*, 6355–6362.
[58] Z. Liu, M.-Z. Zhu, X. Meng, G. Xu, R. Jin, *J. Phys. Chem. Lett.* **2011**, *2*, 2104–2109.
[59] J. Kang, M. Choi, J. Y. Kwon, E. Y. Lee, J. Yoon, *J. Org. Chem.* **2002**, *67*, 4384–4386.
[60] M. Schmittel, H. Lin, *Inorg. Chem.* **2007**, *46*, 9139–9145.
[61] A. S. Al-Kady, M. Gaber, M. M. Hussein, El-Z. M. Ebeid, *J. Phys. Chem. A* **2009**, *113*, 9474–9484.
[62] J. Malicka, I. Gryczynski, J. Kusba, J. R. Lakowicz, *Biopolymers* **2003**, *70*, 595–603.
[63] J. R. Lakowicz, *Anal. Biochem.* **2005**, *337*, 171–194.
[64] K. Aslan, Z. Leonenko, J. R. Lakowicz, C. D. Geddes, *J. Fluoresc.* **2005**, *15*, 643–654.
[65] S. K. Ghosh, T. Pal, *Chem. Rev.* **2007**, *107*, 4797–4862.
[66] A. Ianoul, A. Bergeron, *Langmuir* **2006**, *22*, 10217–10222.
[67] S. Pan, Z. Wang, L. J. Rothberg, *J. Phys. Chem. B* **2006**, *110*, 17383–17387.
[68] Z. Wu, *Angew. Chem. Int. Ed.* **2012**, *51*, 2934–2938.
[69] P. Apell, R. Monreal, S. Lundqvist, *Phys. Scr.* **1988**, *38*, 174–179.
[70] S. H. Cha, J. U. Kim, K. H. Kim, J. C. Lee, *Chem. Mater.* **2007**, *19*, 6297–6303.
[71] M. Zhu, C. M. Aikens, F. J. Hollander, G. C. Schatz, R. Jin, *J. Am. Chem. Soc.* **2008**, *130*, 5883–5885.
[72] T. P. Bigioni, R. L.Whetten, O. Dag, *J. Phys. Chem B* **2000**, *104*, 6983–6986.

Received: December 9, 2011
Revised: January 20, 2012
Published online: April 4, 2012


© 2012 Wiley-VCH Verlag GmbH & Co. KGaA, Weinheim